Supporting Information for the Manuscript

Two pH-directed coordination polymers of cadmium isomers based on a semi-rigid polycarboxylic acid: crystal Structure and fluorescence sensing of tetracyclines

Shaodong Li,[a] Mengzhao Li,[a] Jia Li,[a] Yang Zhang,[a] Feng Su,[a] Longlong Ma,[a] Guangyan Wang,[a] Xinlei Li[a] and Zhijun Wang*[a]

[a]Department of chemistry, Changzhi University, Changzhi 046011, People's Republic of China.

Material and General Methods

H_4dppta was received from Jinan Trading Company, China. All other reagents and solvents were purchased from commercial sources and used without further purification. Various antibiotics including tetracycline (TC), chlortetracycline (CTC), oxytetracycline (OTC), Enoxacin (ENX), penicillin (PCL); cephalexin (CEX), gentamycin (GEN), roxithromycin (ROX); azithromycin (AZI), lincomycin (LCM), sulfadiazine (SDZ), thiamphenicol (TAP) were procured from Aldrich.

The IR spectra were recorded from a KBr pellet in the range of 4000-400 cm^{-1} on a Bruker ALPHA spectrometer. and given in Figure S1. EAs were carried out using a CHNO-Rapid instrument. PXRD data were recorded on a Bruker D8 ADVANCE X-ray diffractometer with Cu−$K\alpha$ radiation (λ = 1.5406 Å) in the range of 5−50° with 2θ at a rate of 5°/min^{-1}. TGAs were carried out on a Dupont thermal analyzer with temperature range of 25−800 °C under N_2 flow with a heating rate of 10 °C min^{-1}. Fluorescence spectra were characterized at room temperature using a Fluorescence spectra of samples were measured using a Thermo scientific LUMINA fluorescence spectrometer at room temperature. The surface features of products were observed using a Zeiss EVO LS 10 scanning electron microscope (SEM), operating with an accelerating voltage of 20 kV. UV-vis spectra were recorded on a HITACHI U-2910 spectrometer. Ultraviolet visible (UV–vis) absorption spectra were recorded with a Hitachi UV-2600 spectrophotometer. Luminescent lifetimes were measured on a

HORIBA FluoroMax fluorescence spectrometer with a microsecond (100 mW) lamp as an excitation source, and lifetime data were obtained by fitting the experimental luminescent decay curves. The fluorescence quantum yields were investigated by Hamamatsu Quantaurus-QY spectrometer. X-ray photoelectron spectroscopy (XPS) was performed on Thermo ESCALAB XI+. Inductively coupled plasma spectrometer (ICP) was performed on AVIO200

X-ray Crystallographic Data Collection and Structural Determination.

After all non-H atoms were refined anisotropically, hydrogen atoms attached to C atoms were placed geometrically and refined using a riding model approximation, with C–H = 0.93 Å and U_{iso}(H) = 1.2U_{eq}(C). H atoms attached to O atoms were located from difference Fourier maps, and their bond lengths and their bond lengths were idealized to lie in the range 0.81 to 0.83 Å, and they were refined using a riding model, with U_{iso}(H) = 1.5U_{eq}(O). Some O atoms of the dppta^{4-} ligand in ***2*** were disordered with relatively irregular ellipsoids and similarity restraints for anisotropic displacement parameters. The topological analyses were performed on the TOPOS program[S1].

Tables S1 Selected bond lengths [Å] and angles [°] for CP-***1***.

CP-***1***			
Cd(1)-O(7)	2.312(4)	N(4)-Cd(1)-O(4)#3	80.09(15)
Cd(1)-O(5)#2	2.345(4)	O(7)-Cd(1)-N(3)	89.36(17)
Cd(1)-N(4)	2.353(5)	O(5)#2-Cd(1)-N(3)	118.22(16)
Cd(1)-O(4)#3	2.380(4)	N(4)-Cd(1)-N(3)	69.05(16)
Cd(1)-N(3)	2.398(5)	O(4)#3-Cd(1)-N(3)	120.16(15)
Cd(1)-O(8)	2.454(4)	O(7)-Cd(1)-O(8)	54.60(13)
Cd(1)-O(4)#2	2.456(4)	O(5)#2-Cd(1)-O(8)	89.04(14)
Cd(2)-O(2)	2.339(4)	N(4)-Cd(1)-O(8)	149.52(15)
Cd(2)-N(2)	2.348(5)	O(4)#3-Cd(1)-O(8)	129.65(14)
Cd(2)-O(2)#4	2.352(4)	N(3)-Cd(1)-O(8)	87.11(15)
Cd(2)-O(10)#1	2.394(5)	O(7)-Cd(1)-O(4)#2	90.80(14)
Cd(2)-N(1)	2.403(5)	O(5)#2-Cd(1)-O(4)#2	54.40(13)
Cd(2)-O(9)#1	2.441(5)	N(4)-Cd(1)-O(4)#3	80.09(15)
Cd(2)-O(1)	2.525(4)	O(7)-Cd(1)-N(3)	89.36(17)
C(15)-O(9)-Cd(2)#1	90.3(4)	O(4)#3-Cd(1)-O(4)#2	72.33(14)
C(15)-O(10)-Cd(2)#1	92.3(4)	N(3)-Cd(1)-O(4)#2	167.38(15)

O(9)-C(15)-O(10)	123.6(6)	O(8)-Cd(1)-O(4)#2	82.72(13)
O(9)-C(15)-C(12)	117.0(6)	O(7)-Cd(1)-C(8)#2	113.73(17)
O(10)-C(15)-C(12)	119.2(6)	O(5)#2-Cd(1)-C(8)#2	27.12(16)
O(10)-C(15)-Cd(2)#1	60.7(4)	O(2)-Cd(2)-N(2)	109.55(15)
C(12)-C(15)-Cd(2)#1	177.0(4)	O(2)-Cd(2)-O(2)#4	71.43(16)
O(7)-Cd(1)-O(5)#2	134.35(14)	N(2)-Cd(2)-O(2)#4	154.03(17)
O(7)-Cd(1)-N(4)	139.37(15)	O(2)-Cd(2)-O(10)#1	90.07(15)
O(5)#2-Cd(1)-N(4)	86.11(15)	N(2)-Cd(2)-O(10)#1	83.27(18)
O(7)-Cd(1)-O(4)#3	82.22(14)	O(2)#4-Cd(2)-O(10)#1	122.59(16)
O(5)#2-Cd(1)-O(4)#3	108.89(14)	O(2)-Cd(2)-N(1)	108.69(17)

Symmetry transformations used to generate equivalent atoms:

#1 -x+1,-y+1,-z #2 x+1,y+1,z #3 -x+1,-y+1,-z+1 #4 -x,-y+1,-z #5 x-1,y-1,z

Tables S2 Selected bond lengths [Å] and angles [°] for CP-***2***.

CP-***2***

Cd(1)-O(9)#1	2.276(4)	O(7)#2-Cd(1)-N(3)	148.01(18)
Cd(1)-O(7)#2	2.278(4)	O(8)-Cd(1)-N(3)	88.95(15)
Cd(1)-O(8)	2.303(4)	O(9)#1-Cd(1)-N(4)	114.82(18)
Cd(1)-N(3)	2.369(5)	O(7)#2-Cd(1)-N(4)	83.97(18)
Cd(1)-N(4)	2.379(5)	O(8)-Cd(1)-N(4)	144.27(16)
Cd(1)-O(6)	2.461(5)	N(3)-Cd(1)-N(4)	69.15(18)
Cd(2)-O(1)	2.214(7)	O(9)#1-Cd(1)-O(6)	163.82(18)
Cd(2)-O(4)#3	2.238(6)	O(7)#2-Cd(1)-O(6)	92.80(15)
Cd(2)-N(2)	2.307(6)	O(8)-Cd(1)-O(6)	77.97(14)
Cd(2)-O(11)	2.312(8)	N(3)-Cd(1)-O(6)	97.77(17)
Cd(2)-N(1)	2.354(6)	N(4)-Cd(1)-O(6)	77.53(19)
Cd(1)-O(9)#1	2.276(4)	O(1)-Cd(2)-O(4)#3	107.0(3)
O(9)#1-Cd(1)-O(7)#2	78.81(15)	O(1)-Cd(2)-N(2)	92.0(3)
O(9)#1-Cd(1)-O(8)	94.85(14)	O(4)#3-Cd(2)-N(2)	150.9(2)
O(7)#2-Cd(1)-O(8)	122.85(16)	O(1)-Cd(2)-O(11)	91.5(3)
O(9)#1-Cd(1)-N(3)	96.56(17)	O(4)#3-Cd(2)-O(11)	97.9(3)

Symmetry transformations used to generate equivalent atoms:

#1 -x,-y+1,-z #2 -x+1,-y+1,-z #3 -x+1,y+1/2,-z+1/2 #4 -x+1,y-1/2,-z+1/2

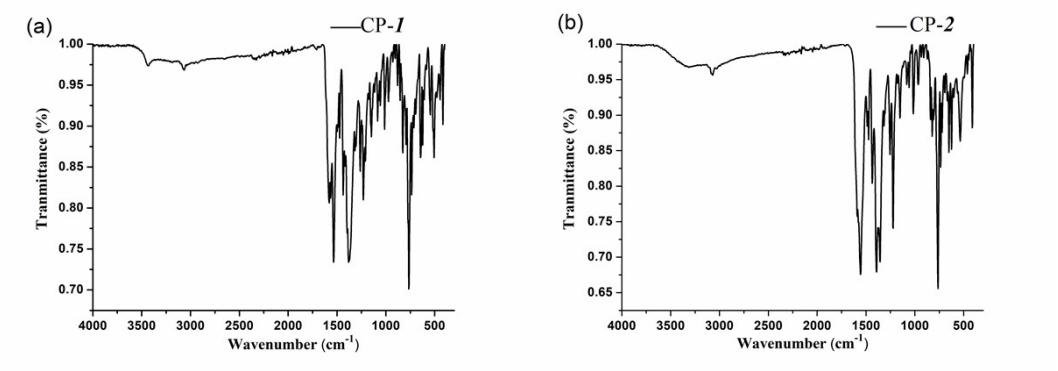

Fig. S1. IR spectra of CP-***1*** and CP-***2*** (KBr, cm^{-1}).

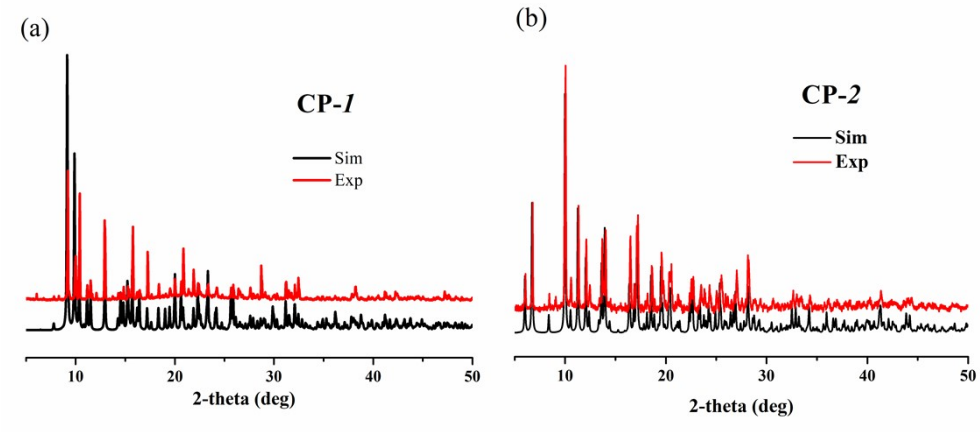

Fig. S2 Comparison of the simulated and experimental PXRD patterns of CP-***1*** and CP-***2***.

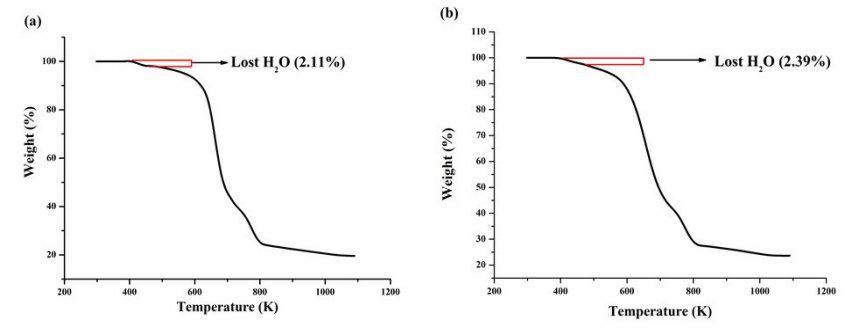

Fig. S3 TGA curves of CP-***1*** (a) and CP-***2*** (b).

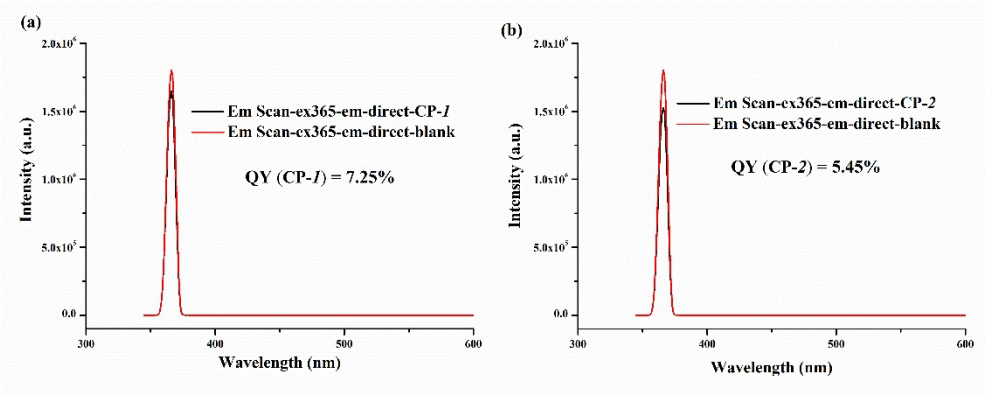

Fig. S4 The luminescent quantum yields of CP-***1*** (a) and CP-***2*** (b).

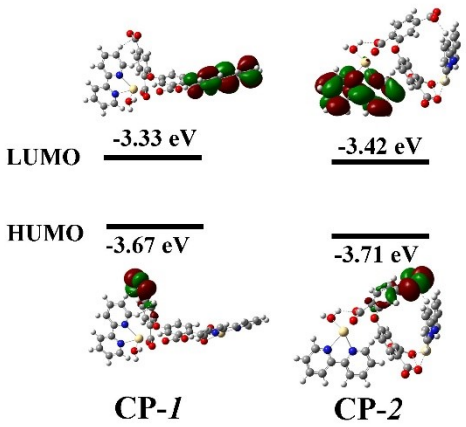

Fig. S5 HOMO−LUMO energy levels of the solid stated of CP-***1*** and CP-***2***.

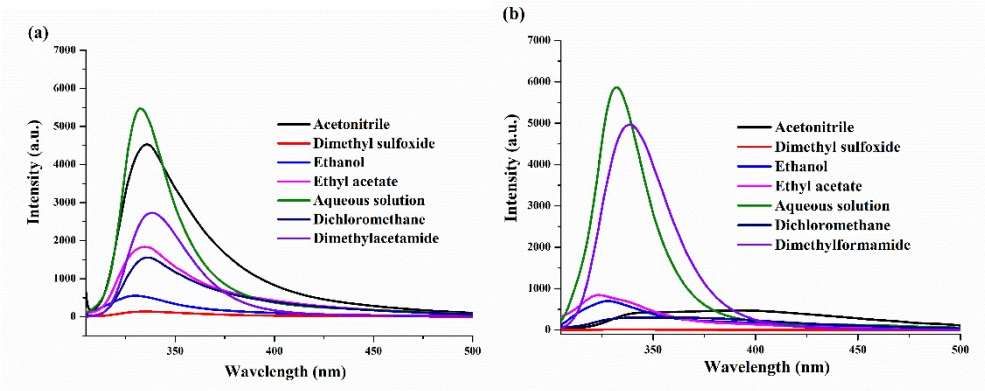

Fig. S6 The luminescence intensities of CP-***1*** (a) and CP-***2*** (b)immersed in different solvents.

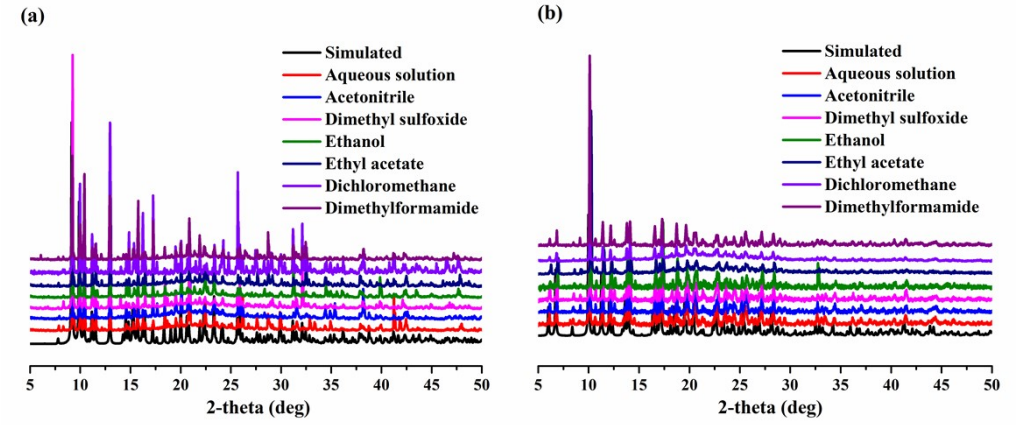

Fig. S7 The PXRD of CP-***1*** (a) and CP-***2*** (b) immersed in different solvents.

Table S3. ICP experiments of CP-***1*** and CP-***2*** after immersing in different solution

Concentration of Cd(II) ions in different solvents (mg/L)	Aqueous solution	Ethanol	N,N-dimethy--lformamide	Acetonitrile	Dichloromethane	Ethyl acetate	Dimethyl sulfoxide
CP-***1***	6.592	0.750	0.220	4.885	0.272	0.131	4.395
CP-***2***	6.998	1.570	0.664	2.781	0.842	0.112	5.961

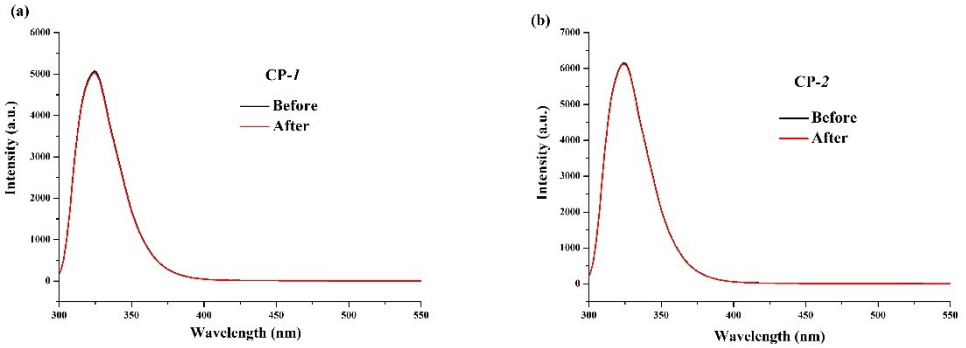

Fig. S8 The fluorescence of the aqueous suspension of the CP-***1*** (a) and CP-***2*** (b) before and after filtration through a 22 μm membrane.

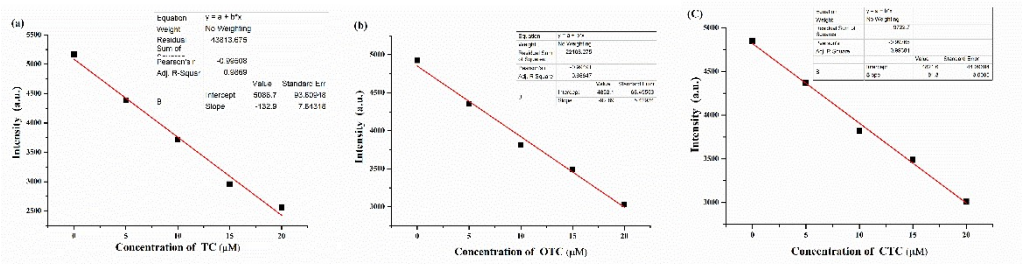

Fig. S9 Linear region of fluorescence intensity of CP-***1*** suspensions in water upon incremental addition 0.001 M of TC, OTC and CTC solutions.

Table S4 Calculation of CP-***1*** Detection Limit for TC, OTC and CTC

Blank Readings	TC	OTC	CTC
Fluorescence Intensity (CP-***1***)	4753	4765	4852
Fluorescence Intensity (CP-***1***)	4764	4769	4850
Fluorescence Intensity (CP-***1***)	4760	4770	4845
Fluorescence Intensity (CP-***1***)	4756	4777	4839
Fluorescence Intensity (CP-***1***)	4769	4775	4849
Standard Deviation (σ)	5.678	4.308	4.604
Slope (m)	132.9	92.9	91.3
Detection Limit (3σ/m)	0.128 μM	0.139 μM	0.151 μM

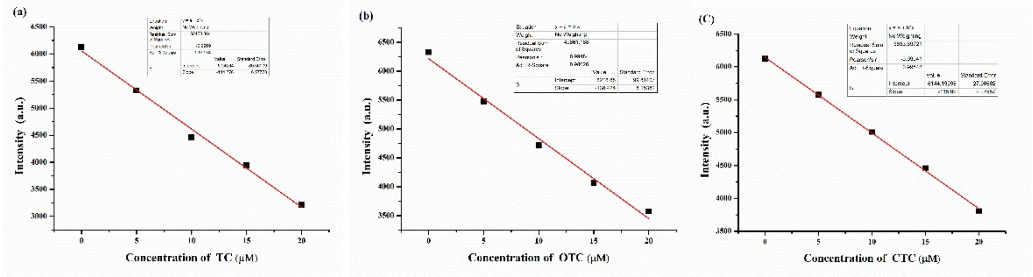

Fig. S10 Linear region of fluorescence intensity of CP-***2*** suspensions in water upon incremental addition 0.001 M of TC, OTC and CTC solutions.

Table S5 Calculation of CP-***2*** Detection Limit for TC, OTC and CTC

Blank Readings	TC	OTC	CTC
Fluorescence Intensity (CP-***2***)	6042	6120	6082
Fluorescence Intensity (CP-***2***)	6012	6135	6054
Fluorescence Intensity (CP-***2***)	6060	6159	6076
Fluorescence Intensity (CP-***2***)	6020	6148	6063
Fluorescence Intensity (CP-***2***)	6014	6171	6094
Standard Deviation (σ)	18.56	17.85	14.06
Slope (m)	144.2	128.4	115.0
Detection Limit (3σ/m)	0.386 μM	0.417 μM	0.367 μM

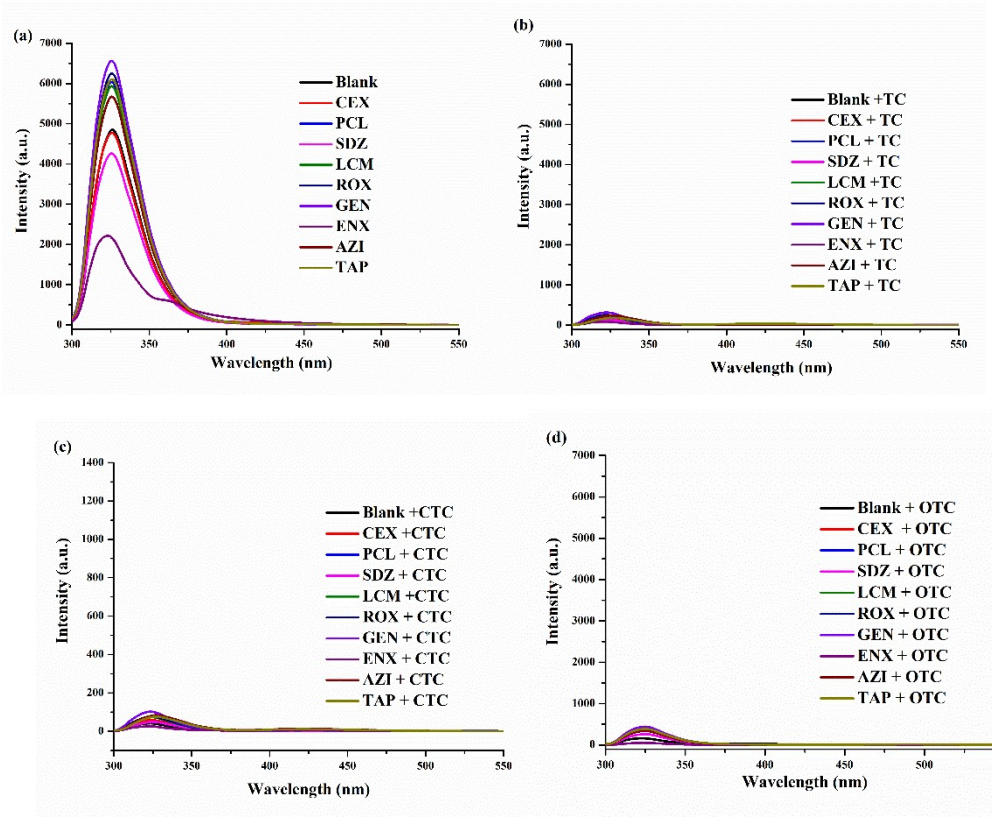

Fig. S11 Emission spectra of CP-***1***: a) adding different antibiotics; b) adding different antibiotics and TC; c) adding different antibiotics and CTC, d) adding different antibiotics and OTC.

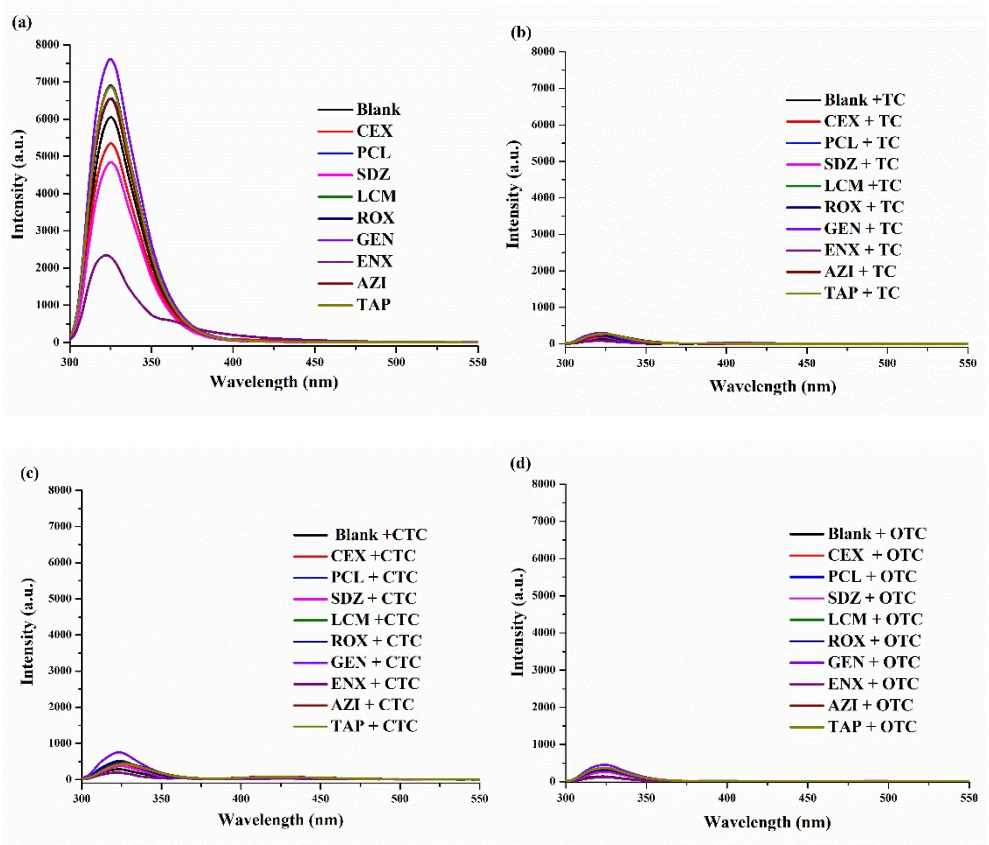

Fig. S12 Emission spectra of CP-***2***: a) adding different antibiotics; b) adding different antibiotics and TC; c) adding different antibiotics and CTC, d) adding different antibiotics and OTC.

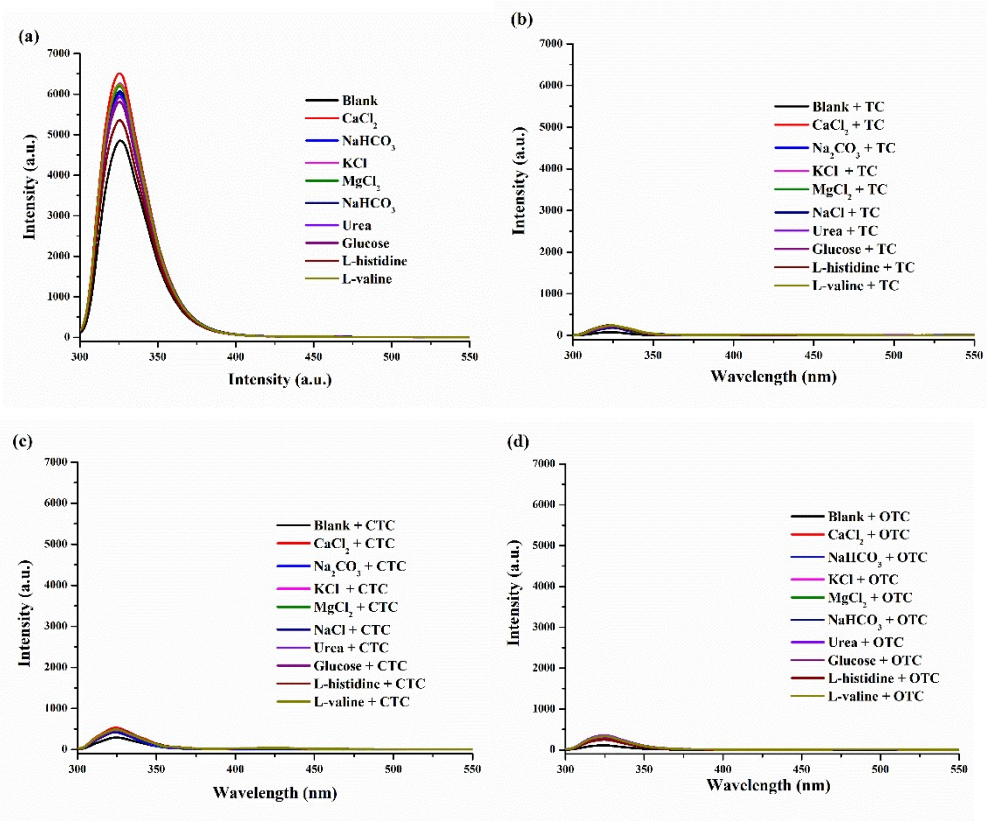

Fig. S13 Emission spectra of CP-***1***: a) adding different blood compositions; b) adding different blood compositions and TC; c) adding different blood compositions and CTC; d) adding different antibiotics and OTC.

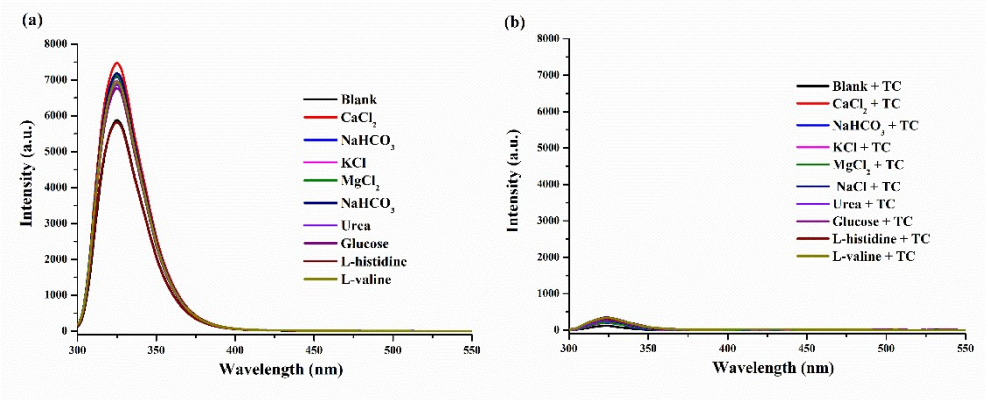

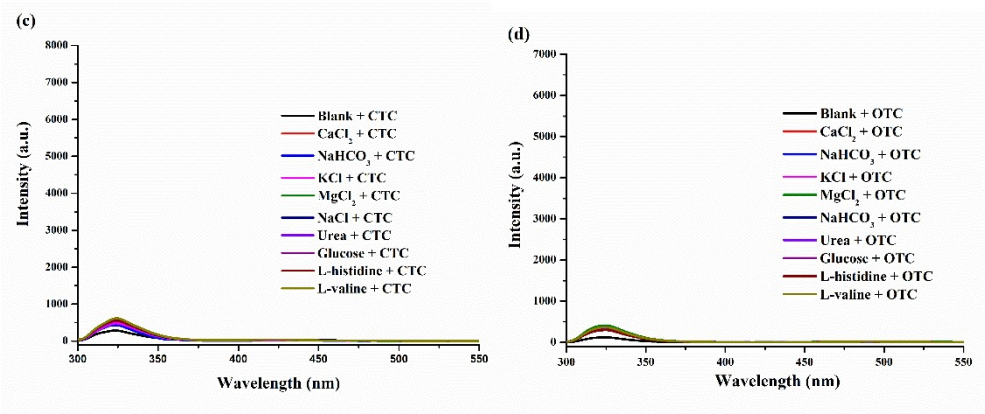

Fig. S14 Emission spectra of CP-*2*: a) adding different blood compositions; b) adding different blood compositions and TC; c) adding different blood compositions and CTC; d) adding different antibiotics and OTC.

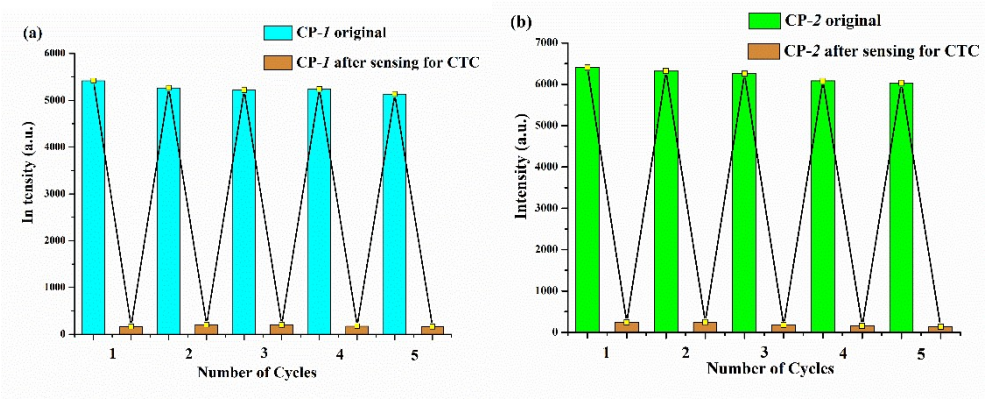

Fig. S15 Recyclability tests for the CTC with CP-*1* (a) and CP-*2* (b).

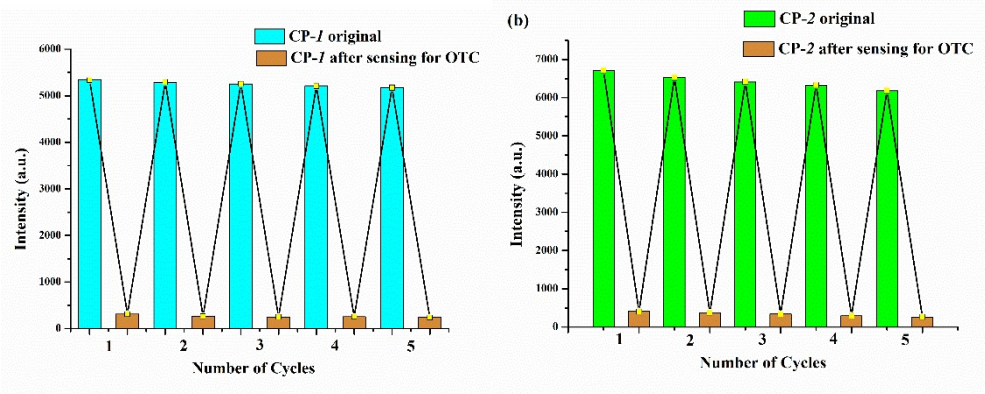

Fig. S16 Recyclability tests for the OTC with CP-*1* (a) and CP-*2* (b).

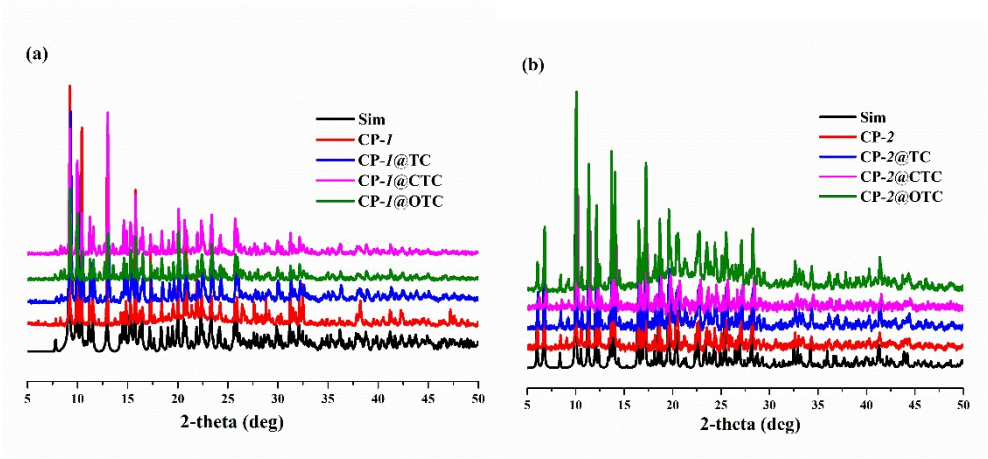

Fig. S17 The PXRD patterns of simulated CP-***1*** (a) and CP-***2*** (b) and the PXRD patterns of CP-***1*** (a) and CP-***2*** (b) for the recognition of TC, CTC and OTC after five recycling processes.

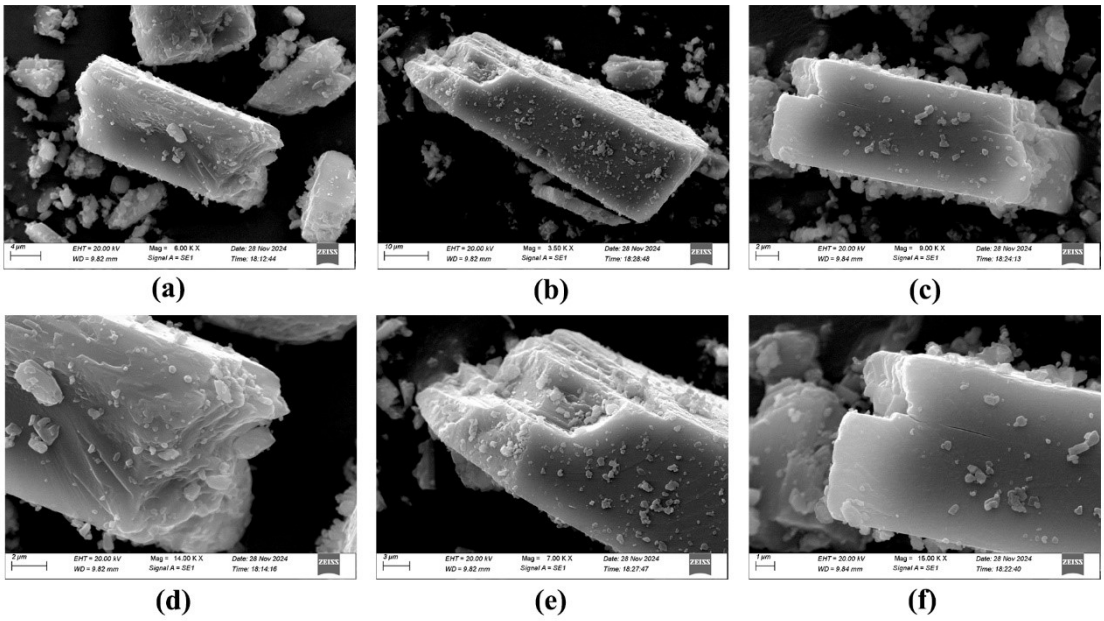

Fig. S18 The SEM patterns of CP-***1*** for the recognition of TC (a,d), CTC (b,e) and OTC (c,f) after five recycling processes.

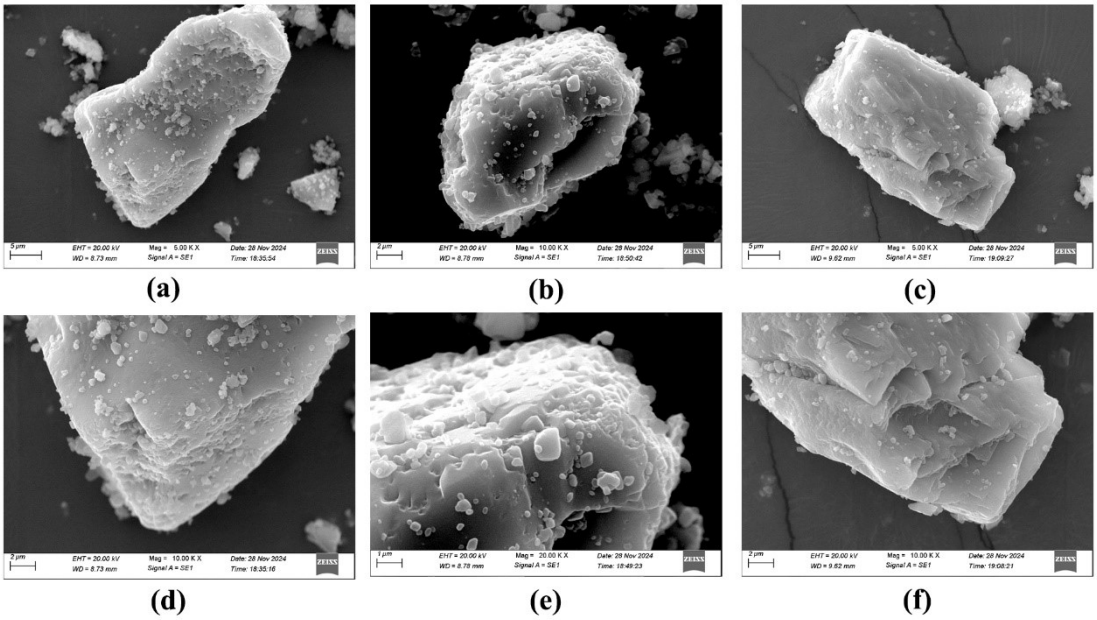

Fig. S19 The SEM patterns of CP-***2*** for the recognition of TC (a,d), CTC (b,e) and OTC (c,f) after five recycling processes.

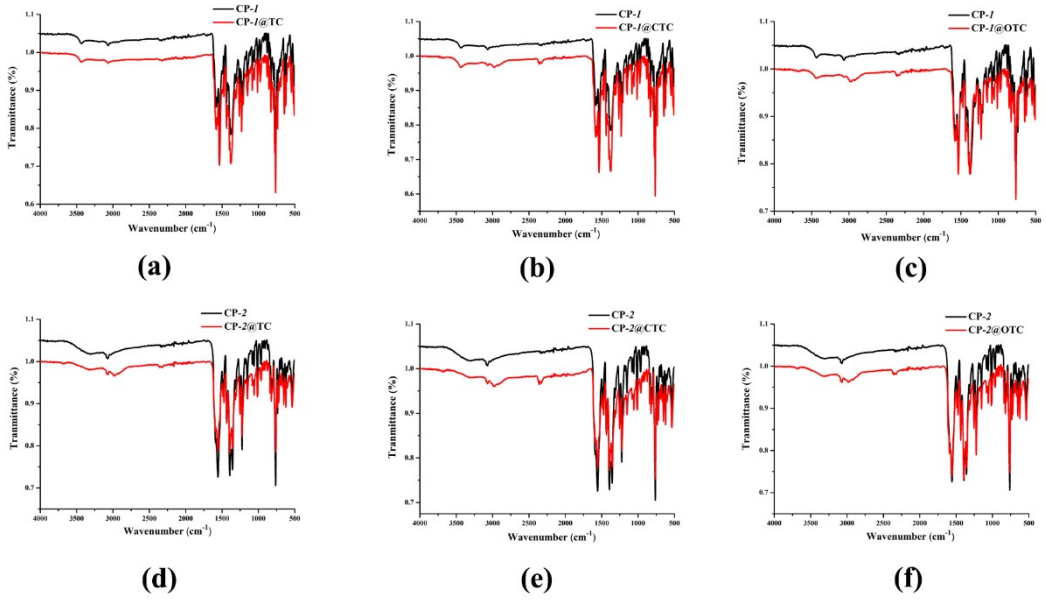

Fig. S20 The IR patterns of CP-***1*** and CP-***2*** for the recognition of TCs after five recycling processes.

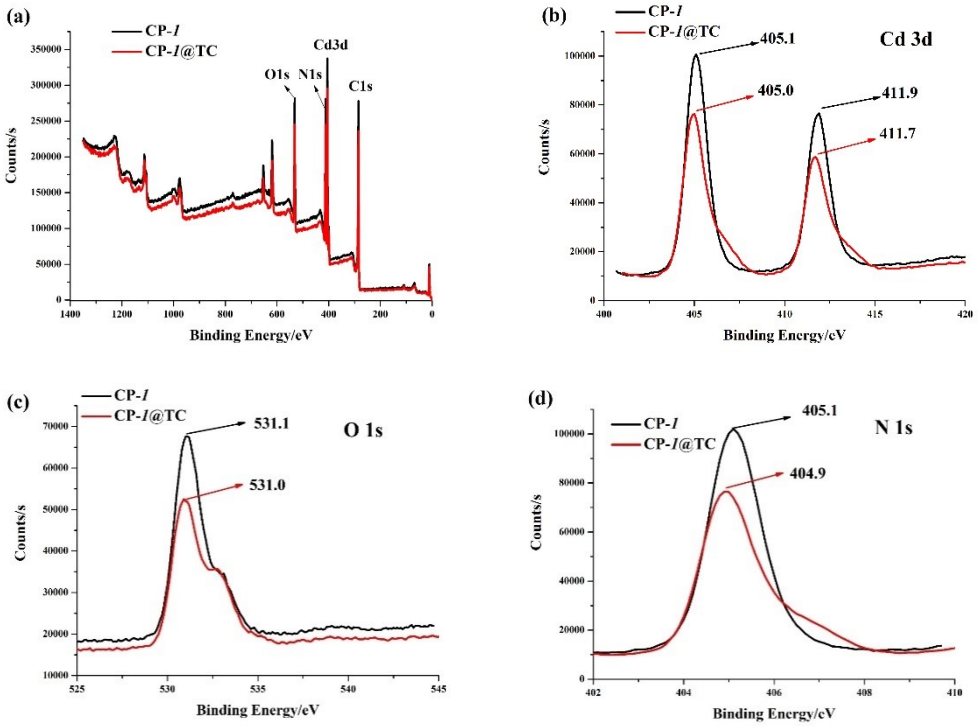

Fig. S21 (a) XPS of CP-***1*** before and after immersion in solutions of TC. The spectra of (b) Cd 3d, (c) O1s and (d) N 1s.

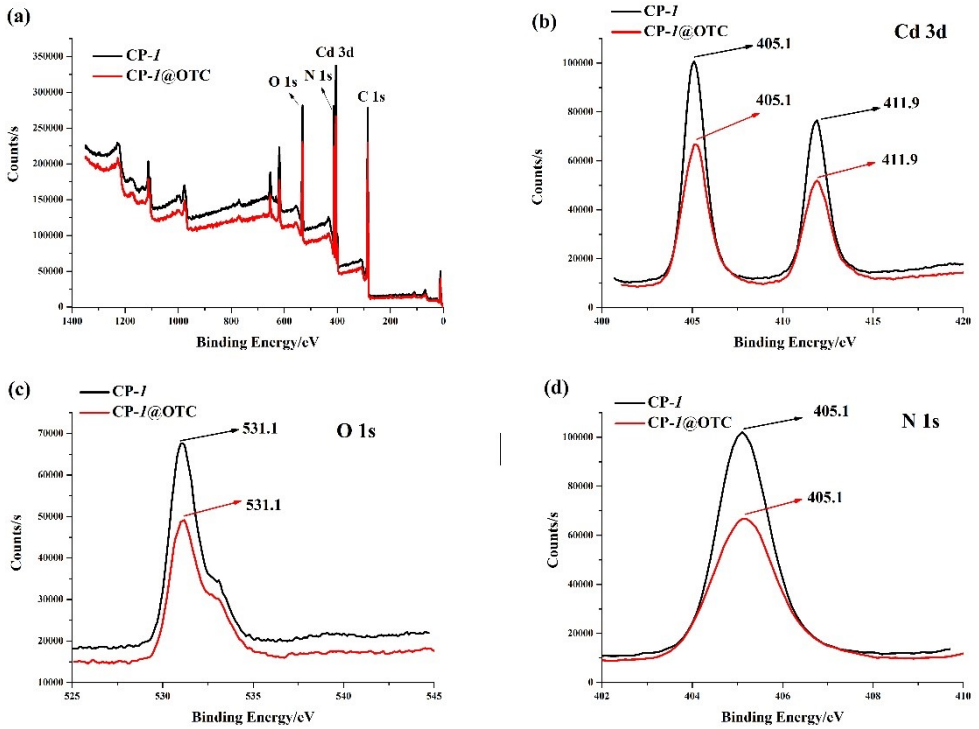

Fig. S22 (a) XPS of CP-***1*** before and after immersion in solutions of OTC. The spectra of (b) Cd 3d, (c) O1s and (d) N 1s.

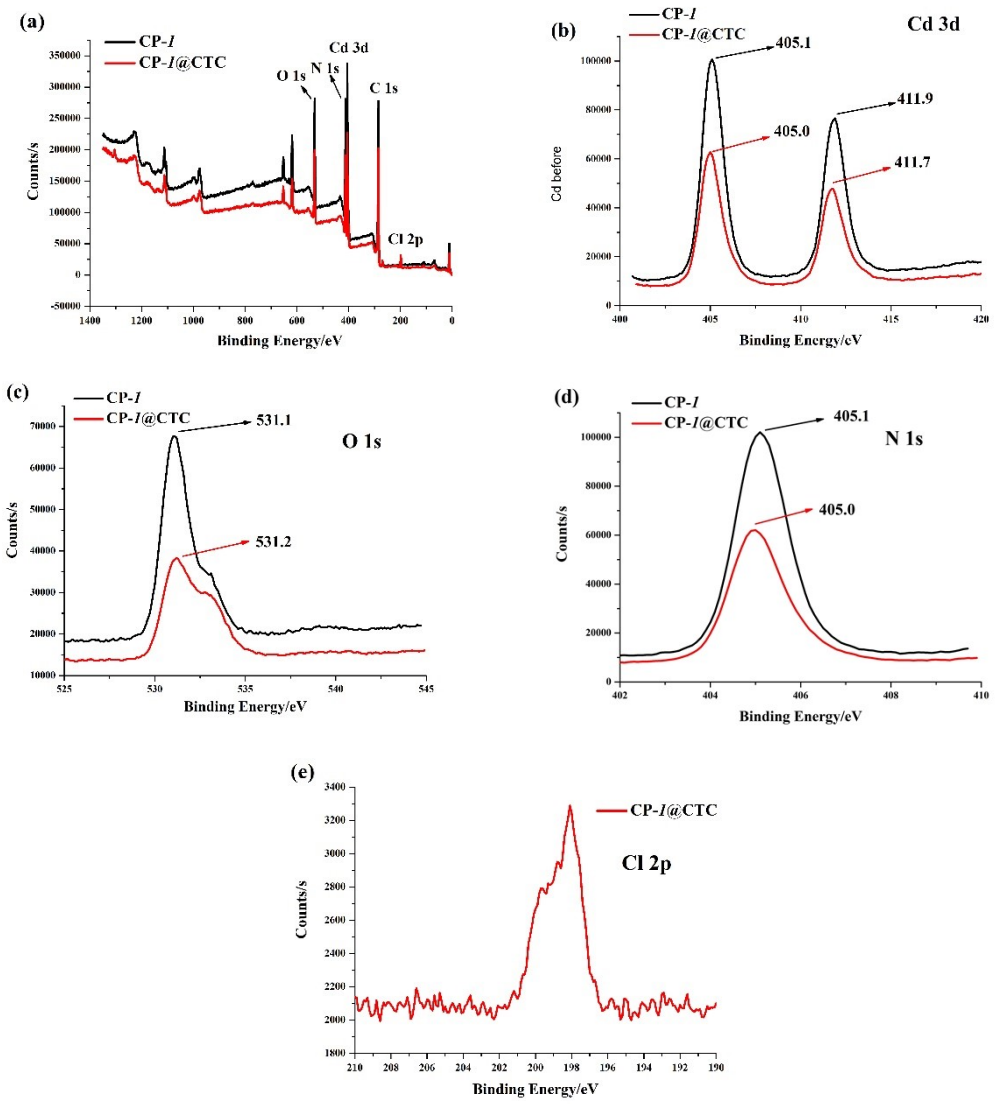

Fig. S23 (a) XPS of CP-*1* before and after immersion in solutions of CTC. The spectra of (b) Cd 3d, (c) O1s, (d) N 1s and (e) Cl 2p.

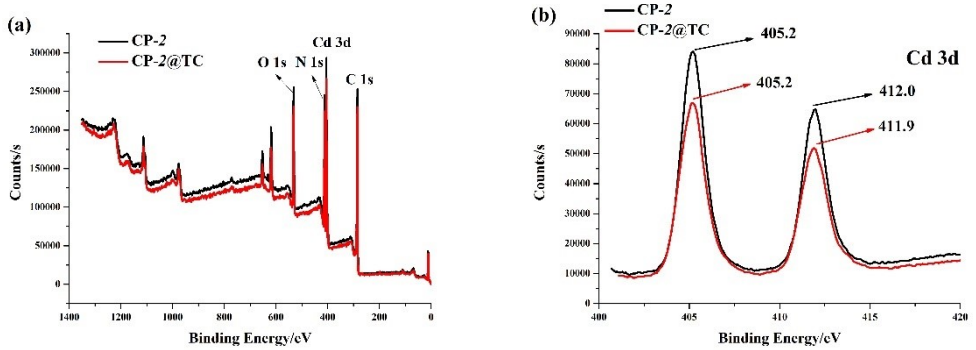

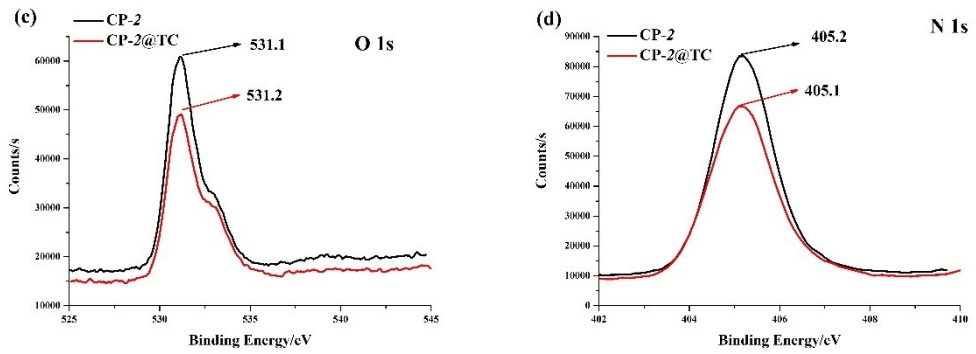

Fig. S24 (a) XPS of CP-***2*** before and after immersion in solutions of TC. The spectra of (b) Cd 3d, (c) O1s and (d) N 1s.

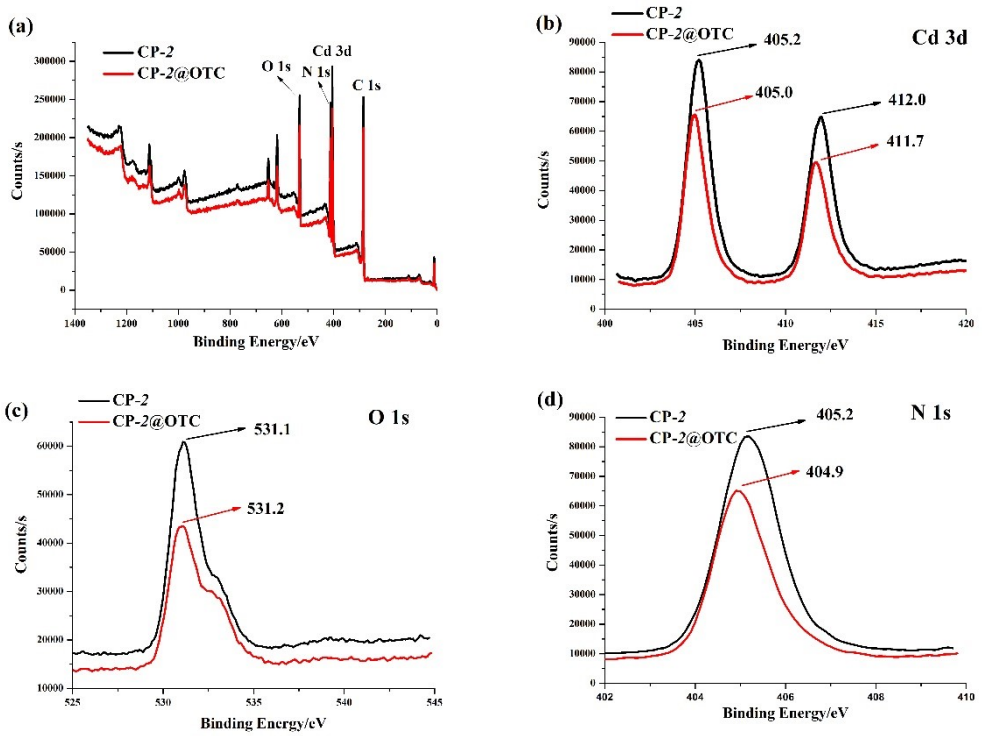

Fig. S25 (a) XPS of CP-***2*** before and after immersion in solutions of OTC. The spectra of (b) Cd 3d, (c) O1s and (d) N 1s.

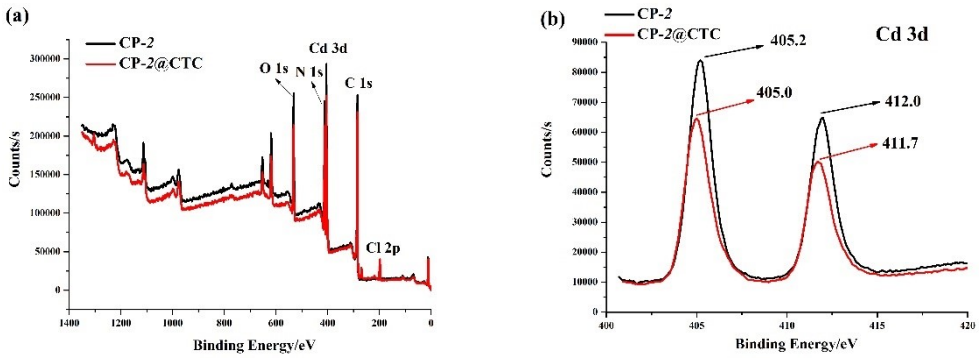

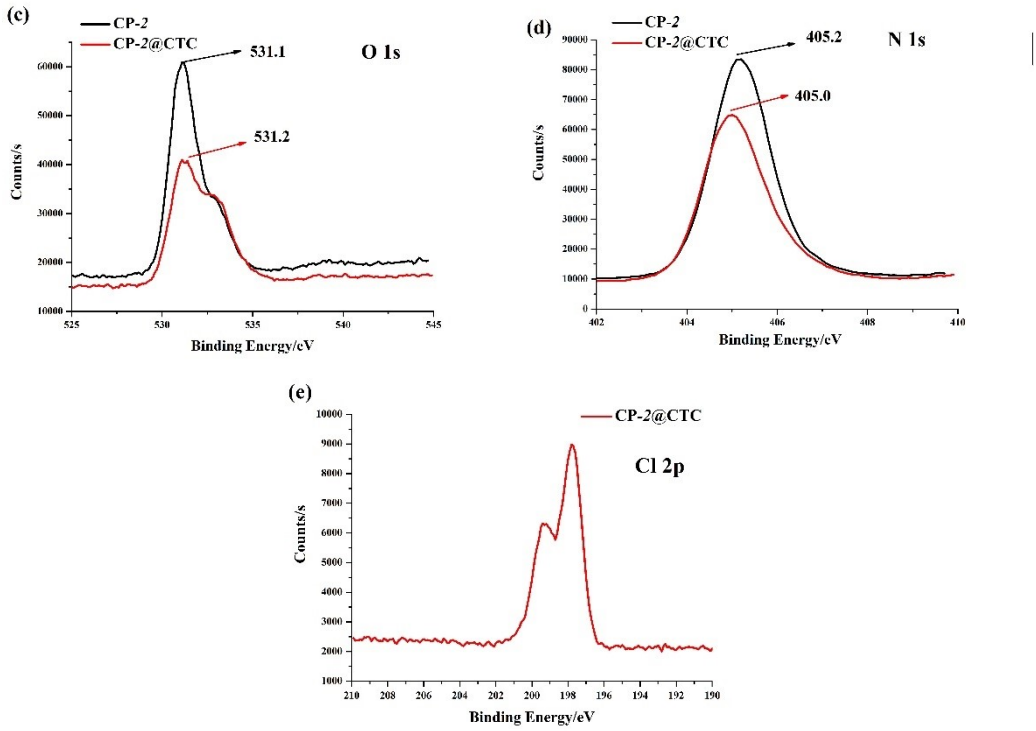

Fig. S26 (a) XPS of CP-***2*** before and after immersion in solutions of CTC. The spectra of (b) Cd 3d, (c) O1s, (d) N 1s and (e) Cl 2p.

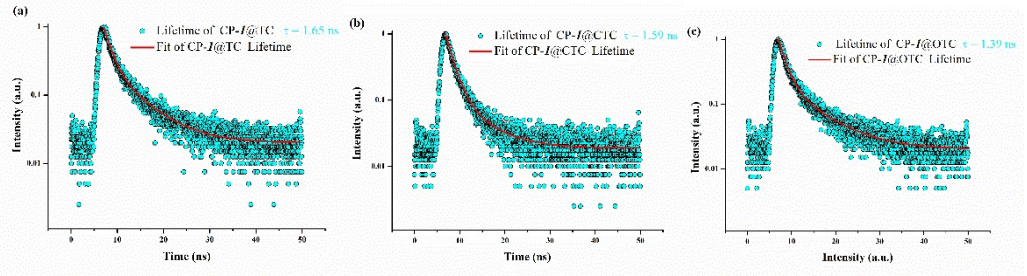

Fig. S27 The luminescence lifetime of CP-***1*** for the recognition of TCs after five recycling processes.

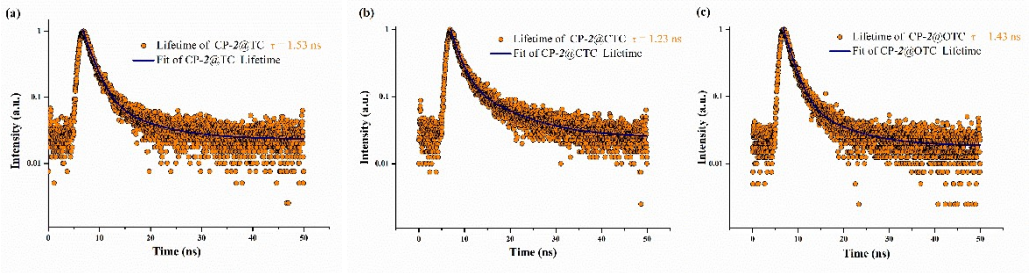

Fig. S28 The luminescence lifetime of CP-***2*** for the recognition of TCs after five recycling processes.